

# Improving Signal Stability in a Multi-Electrode Array (MEA) System for Cardiac Biopsies

Antonio Velarte, Aránzazu Otín, Esther Pueyo  
Instituto de Investigación en Ingeniería de Aragón (I3A)  
Universidad de Zaragoza  
Zaragoza, Spain  
{avelarte, aranotin, epueyo}@unizar.es

Anton Guimerà, Rosa Villa  
Instituto de Microelectrónica de Barcelona  
Centro Nacional de Microelectrónica  
Barcelona, Spain  
{anton.guimera, rosa.villa}@imb-cnm.csic.es

**Abstract**—This work evaluates the performance of a microelectrode array (MEA) to be used in a specific platform dedicated for measuring field potentials of small human cardiac samples. A test bench has been developed to characterize the electrodes by measuring their impedance as well as to modify their characteristic curve using a replatinization process, where black platinum is deposited on the indicated areas of the MEA flex-pcb. This set-up consists of the array of microelectrodes made of gold, together with its corresponding electronic adapter board, a potentiostat and an electrochemical interface. Phosphate buffered saline (PBS), which is commonly considered for this type of analysis, has been used for impedance characterization. Initially, the impedance presents a highly variable behavior at different frequencies as well as between the different channels of the array. Once the platinization process has been carried out, the impedance in all the recording channels is very similar and has decreased over a large part of the frequency range under study. A complete electrical model of the electrodes has been proposed and analyzed, achieving better results by including the mathematical constant phase element (CPE) associated with capacitive behavior (model fitting error < 2%). Finally, the characterization of the different noise contributions has been carried out. Based on the obtained results, it can be concluded that the evaluated system allows the recording of field potential signals from small human cardiac tissues.

**Index Terms**—Multi-Electrode Array (MEA), Human Cardiac Slice, Electrochemical Impedance Spectroscopy (EIS), Electrode coating, Signal Noise Ratio (SNR)

## I. INTRODUCTION

Monitoring of the electrical activity of the heart is of interest for the investigation of cardiac diseases and the development of new therapeutic strategies. Recent advances in electrophysiological recording techniques have led to the development of new tools and equipment for the acquisition and processing of multiscale cardiac electrical activity. Multi-electrode arrays (MEA) have been used to record electrophysiological signals due to their ability to simultaneously monitor signals at different spatial locations [1]. This technique is well developed in the neural domain, where it is used to measure complex neural networks cultured *in vitro* or for *in vivo* applications.

Based on the advantages of MEA, its use has been extended to other research fields, such as cardiac activity recording, either applied to stem cell-derived cell cultures [2] or animal and human tissue slices [3]. In the cardiac field, MEA

recordings are chosen based on the balance between accuracy and performance [4]. An application that generates great interest is the use of MEA for the characterization of drug-induced effects in tissues [5]. Although MEAs are becoming more widely used in electrophysiology laboratories, they are not always easily adapted to the requirements of a specific investigation or their cost is too high [6]. The present work is framed in a research line that involves the development of a MEA-based system to record field potentials (FP) from human cardiac samples in *ex vivo* experiments. The obtained results will contribute with new knowledge regarding the electrical activity of human cardiac tissue slices that adequately preserve all the structural and functional properties of the tissue [7].

The main goal of our work was to design a platform that allows recording electrical FP from small cardiac biopsies, for which it is essential that the system performs the measurements as accurately as possible. Here, we improved the stability of the recorded signals, which is one of the key tasks in this type of systems. We identified the different sources of noise that appeared along the recording chain, such as thermal noise or the intrinsic noise of the recording amplifiers, in order to reduce the total noise of the system. Additionally, it is very important to avoid signal attenuation by ensuring that the impedance of the electrode is much lower than the one associated with the recording amplifier, since a voltage divider is created between them, which couples the signal from the tissue to the input of the operational amplifier. This divider is shown in Fig. 1, where  $Z_a$  represents the input of the amplifier,  $C_p$  accounts for all the shunt capacitance to ground that appears along the recording chain and  $Z_{el}$  is the equivalent circuit model of a metal microelectrode for electrophysiological signal acquisition [8].  $Z_{el}$  comprises the resistance of the electrolyte solution ( $R_s$ ), the resistance and capacitance at the double layer interface electrode-electrolyte ( $R_{el}$  and  $C_{el}$ ), detailed in section II-B, and the resistance of the metal electrode ( $R_m$ ), negligible due to its low value [9].

The electrodes considered in the setup have been characterized and the replatinization process has been carried out to adjust the impedance to the desired values, thus reducing the intrinsic noise of the electrodes, related to the real part of the electrode impedance [10]. This impedance reduction also aims to minimize the attenuation of the signal due to the

voltage divider between the electrode and the amplifier.

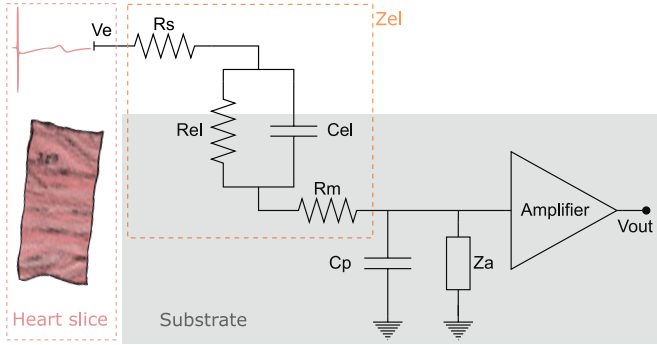


Fig. 1. Signal path of the signal from the cardiac tissue to the amplifier (adapted from [8]). The equivalent circuit model of a metal microelectrode is boxed in orange. Pink box indicates that FP comes from a cardiac tissue slice (extracted from [11]).

The experimental configuration to be used in the electrophysiology laboratory has been set up by an adequate design of the different masses and references distribution, leading to minimization of the influence of the existing noise in the working environment on the obtained signal. A Faraday cage has been also considered in the setup to reduce the electromagnetic noise. The obtained results confirm that the setup is ready to collect FP signals from slices of small cardiac tissues obtained from human biopsies.

## II. CHARACTERIZATION PROCEDURE AND EXPERIMENTAL SETUP CONFIGURATION

This section describes the devices used to perform the characterization and replatinization process of the electrodes in MEAs. Also, it presents a brief explanation of the double-layer model and how to obtain the most relevant parameters of the electrical model considered for this type of electrodes. Finally, a description of the laboratory setup that will be considered in the next steps of the research for the acquisition of FPs from the cardiac samples is included.

### A. Characterization and platinization setup

The microelectrode array has been designed and fabricated at the Institute of Microelectronics of Barcelona (IMB-CNM-CSIC) and consists of sixteen  $50 \mu\text{m}$  measurement points with a distance between them of  $125 \mu\text{m}$  [12]. These sizes have been selected based on the requirements of a particular application, in which small cardiac samples are involved. With these dimensions, recordings with a good temporal and spatial resolution are expected to be obtained, which will provide detailed information about the origin and propagation of excitation in cardiac tissue.

The considered setup to measure the impedance and to do the platinum deposition on the electrodes is composed of Solartron 1287 Electrochemical Interface and the potentiostat Solartron 1260, both controlled by the incorporated commercial software (Zplot for characterization and CorrWare for platinization). To verify the correct behavior of the system,

two different discrete resistors, with values of  $10 \text{ k}\Omega$  and  $330 \text{ k}\Omega$ , were measured in a frequency sweep from  $100 \text{ Hz}$  to  $1 \text{ MHz}$ , considering the errors according to the measuring range indicated by the manufacturer. The values of the resistances are selected on the basis of the limitations of the measurement devices.

An initial check of the state of the electrodes was made with an optical microscope to verify that the electrodes had been manufactured properly and that the passivation of the tracks was adequate. The same microscope was used to check that the platinum deposition took place in the measurement areas once the coating process had been completed.

For the impedance measurement, a two-point configuration was used and a sine wave of  $10 \text{ mV}$  amplitude with frequencies ranging from  $0.1 \text{ Hz}$  to  $10 \text{ MHz}$  was applied. The MEA was placed on a beaker next to a platinum electrode with a larger surface area, which acts as a counter electrode (CE) or reference. In the beaker, a  $10 \text{ mM}$  phosphate buffered saline (PBS) was added until all electrodes were covered. The measurement of each of the MEA channels was performed by manually changing the selected channel, which acts as the working electrode (WE). A picture of the setup can be seen in Fig. 2a.

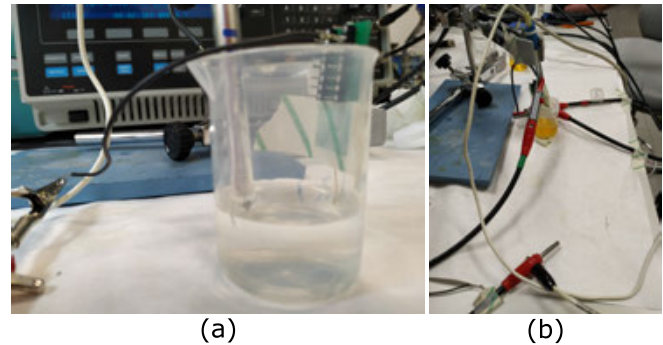


Fig. 2. (a) Setup considered for the impedance measurement, where MEA is immersed in the PBS. (b) Platinization setup.

Black platinum was chosen for platinization, a material suitable for the type of electrodes and this particular application, as it is economical and offers good performance [13]. The preparation of the platinization solution has the following composition:  $0.1 \text{ M}$  hydrochloric acid, platinum chloride and a small amount of lead acetate. In this case, the setup is slightly modified with respect to the characterization setup, separating what is known as the reference electrode from the CE. The CE acts as a current sink and the reference electrode is responsible for sensing the voltage in the liquid. Here, we chose a silver electrode as the reference and a platinum electrode as the CE.

To carry out the process, a beaker was prepared with the solution and the electrode array was placed inside the liquid. In this procedure, all the channels to be modified were short-circuited to ensure that the platinum was deposited properly and uniformly (Fig. 2b), with all the selected channels acting as a single WE. A constant voltage was applied for a few

seconds until the curve showed that the process had been completed.

### B. Electrical model of the electrode-electrolyte interface

An electrode is the physical interface between technological equipment and the biology itself. Whenever a metal electrode is immersed in an electrolyte, chemical reactions begin occurring at the interface, creating a layer of solubilized ions in the electrolyte. This coupled with the fact that the electrode surface forms one half of a plate capacitor, the effect known as double-layer capacitance is formed. To properly understand the charge transfer processes occurring at the interface, a model that incorporates this capacitive behaviour is used (Fig. 1). Based on similar work, two ways of modeling are proposed, a simpler one based on physical elements such as resistors or capacitors, and another one that includes an element known as constant phase element (CPE). This element modeling a specific behavior determined by a mathematical equation similar to that of a capacitor (equation (1)), representing the diffusion limited and roughness terms in the surface impedance. In this work, a comparison has been made between the two types of models in order to evaluate which one fits better to our MEA device.

$$Z_{CPE} = Q_0^{-1}(j\omega)^{-\alpha} \quad (1)$$

In the above equation, two constants ( $Q_0$  and  $\alpha$ ) were considered that can be obtained experimentally. In the case of  $\alpha$ , if it is equal to 1, the behavior of the component is a pure capacitance and if  $\alpha$  is equal to 0, its behavior is purely resistive.

$R_e$  is included in parallel in both models of Fig. 5 to represent the resistive part of the double electric layer. In series with these elements, a resistor  $R_s$  was included that models the contribution of the existing electrolyte between the CE and the WE. Note that a capacitance could also be included to model the phase boundary in the CE, but it was not considered in this particular case because the surface area of the CE had been selected to be much larger than the one of the WE.

At low frequencies, it can be observed that the effect of the CPE is dominant, giving the electrode a capacitance character. This capacitance is directly proportional to the contact area of the electrode with the saline solution, so the impedance curve will decrease with increasing surface area. However, at higher frequencies, the electrical signals begin to flow through the CPE, until the curve becomes flat, where the contribution of  $R_s$  is dominant [14].

### C. Experimental setup required for ex-vivo measurements

The configuration of an electrophysiology system should allow obtaining accurate signals. Here, the focus is to acquire FPs from slices of cardiac biopsies, which should be electrophysiologically evaluated shortly after they have been obtained.

In an electrophysiology laboratory, a large amount of equipment that makes use of the electrical network is present and

generates its corresponding electromagnetic noise. This specially affects the required measurements due to the low signal levels, which can be easily contaminated by the artefacts that these devices can generate or those coming from the network itself. To improve this, an isolated excitation source was used to stimulate the cardiac samples; a correct configuration of the references and masses of the acquisition equipment was established; and a Faraday cage was used to remove the components of the electromagnetic noise from the recordings.

### D. Noise and signal-noise ratio (SNR)

Noise in the extracellular recordings refers to all signal contributions that interfere with the signal of interest. The main types of noise that affected were thermal noise from the electrodes and injected noise from the acquisition system, mainly the noise from the recording amplifiers. Therefore, the quality of the FP recordings and their signal-to-noise ratio was determined by the quality of the signal of interest, obtained in the presence of all these sources of noise, which appear along the different stages that make up the recording system.

## III. RESULTS

### A. Electrode characterization

Two different MEAs of 16 channels (Fig. 6) were used in this work and electrodes made of gold on flexible substrate were characterized. In the measurement procedure, small amplitude signals were applied to avoid unwanted irreversible electrochemical changes at the phase boundary [15]. The platinization process was applied on half of the channels, which allowed us to do a precise comparison.

#### 1) Contribution of the electrolyte:

The first experiment consists of measuring the impedance of the MEA using the setup described in section II. The obtained results with any of the electrodes selected from the two MEAs were similar, so the results from one of them are included as examples (1 and 16 in Fig. 3). The obtained Bode plot (Fig. 3) is the typical for a metal electrode in saline, a high-pass filter.

With the impedance curve it is possible to obtain the contribution of the electrolyte ( $R_s$ ). In the high frequency range, the signals pass through the capacitance  $C_{el}$  (Fig. 1) and the main contribution of the circuit is  $R_s$ , so signals at these frequencies are attenuated by the value of this resistor. To verify that the value of the flat zone reached by the curve is mostly dependent on the considered electrolyte, as stated in [16], different experiments with different types of electrolyte were required. Here, the concentration of the PBS was changed and the obtained responses for 5 and 10 mM were compared. This test verified that the impedance of the electrodes to signals of a high frequency range depended on the employed liquid, being around 6.5 k $\Omega$  in the case of 10 mM PBS (Table I) and 10 k $\Omega$  in the case of 5 mM PBS.

#### 2) Complete model with CPE vs simplified model:

The electrical model of the MEA was adjusted with the obtained data associated with the 10 mM PBS, the electrolyte that will be used in future work. The Zview software was

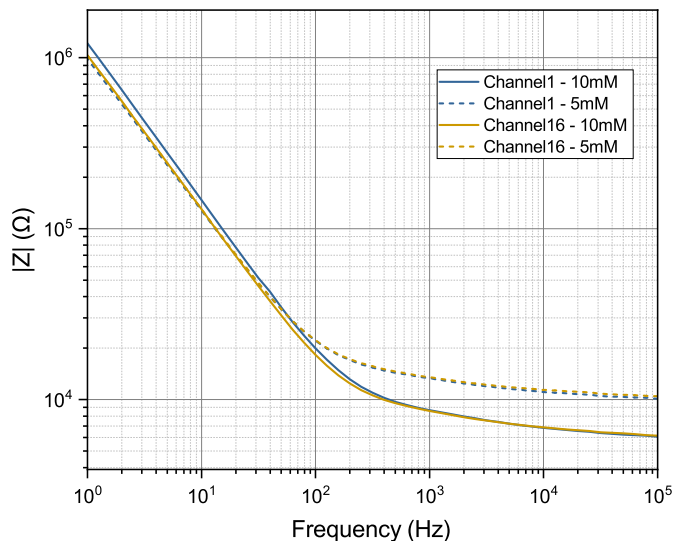


Fig. 3. Comparison of the results obtained using different concentrations of PBS.

used. Two different electrical models were proposed to adjust the impedance of the electrodes and to make a comparison between them (Fig. 5). The first one was a simple model that incorporated physical elements only and the second one made use of the specific component based on mathematical behavior, named as CPE. Fig. 4 shows the results obtained for one of the measurement channels, which is representative given the similarity of the results obtained for the complete set of electrodes.

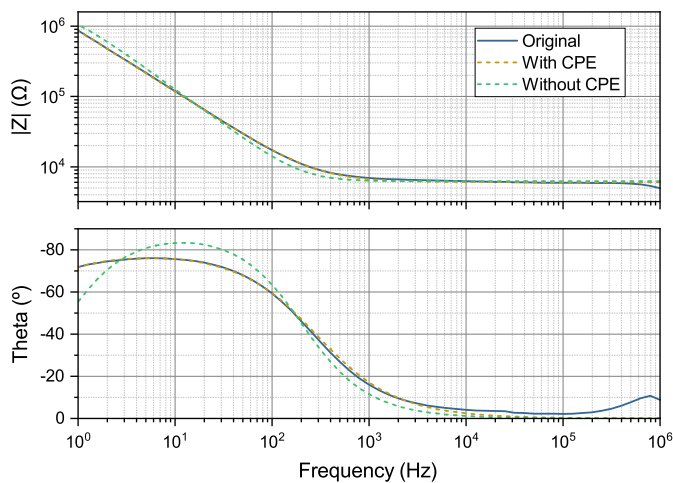


Fig. 4. Comparison of the fitting results obtained using different models, one with the CPE element and another without it.

The fitting results showed more accurate values when using the CPE element, as expected since the electrode curve at low frequencies did not fit exactly to a pure capacitance. The percentage error of the results in this case was very low ( $< 2\%$ ), thus allowing to conclude that this model can be used as a good simulator of the MEA behavior. The  $R_s$  value corresponding to the electrolyte had practically the

same value for both models, confirming that this parameter is independent of the electrode capacity. In the model that incorporates the CPE, the following values for the constants of the model described in Methods were obtained:  $\alpha=0.88267$  and  $Q_0=2.221E-7$ . Since the value of alpha was very close to one, the CPE element behavior was highly capacitive, which explains why the basic model has a very good fit too.

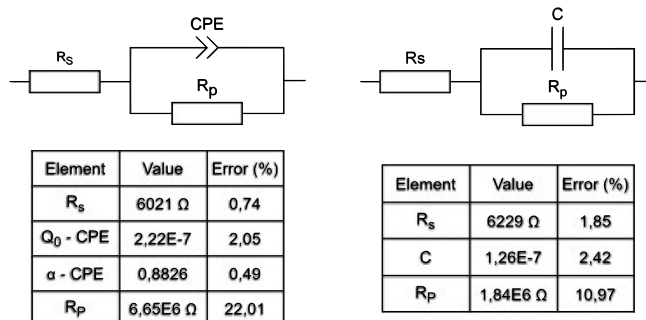


Fig. 5. Electrical models proposed to perform the fitting and values obtained in each situation.

### 3) Modification of the characteristic curve by deposition process:

According to the impedance curves of the MEAs, it is necessary to carry out a process that reduces the impedance of the electrodes, shifting the curve towards lower frequencies. A platinization process was performed by electrochemically coating the electrodes with a layer of black platinum. Results for the electrodes after platinization are shown in black on the left side of Fig. 6 and the gold electrodes are shown in yellow. An enlargement of a specific area is shown, in which the passivation of the tracks is verified, as shown by the difference in color between the measuring point and the tracks, both parts made of gold.

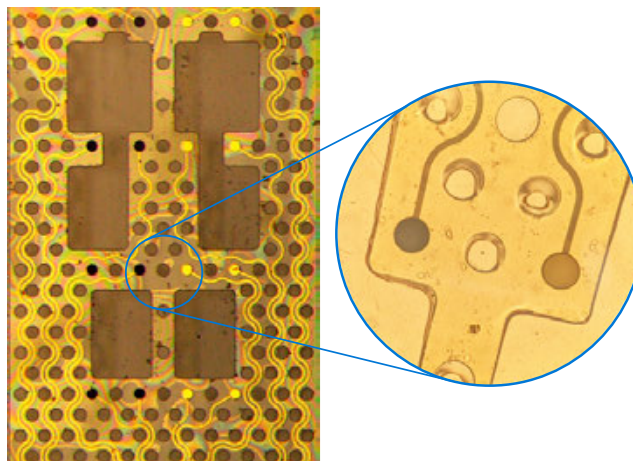


Fig. 6. MEA seen under microscope view. An enlargement of an area showing the difference in colour between the original electrodes and those coated with black platinum is included.

Fig. 7 shows the comparison of the impedance curves obtained before and after platinum deposition. Only the results

of three randomly selected channels were included in the graph, being the results obtained for other channels very similar. The transition of the curve was shifted to the left, so the flat response of the MEA started at lower frequencies, as required. Therefore, the channels showed a more similar behavior with respect to the dispersion that can be seen in the response of the electrodes when only the gold surface is in contact with the electrolyte, an important fact when performing measurements with this type of devices. The impedance shown by the coated electrodes was lower due to the fact that with the same planar area they had greater roughness and therefore greater capacity, which can be seen in the phase rise of the phase diagram (Fig. 7). The phase will never reach the value of  $-90^\circ$  because it is not a pure capacitance. The CPE value will depend on the roughness acquired after coating process, which is usually around  $-70^\circ$  or  $-80^\circ$ .

A typical value that can serve as a reference, which appears in published works with MEA, is the impedance measurement at 1 kHz and how much it has changed after platinization [16]. In our devices, the average initial value of the channels was  $218 \text{ k}\Omega$  and the current value is  $10 \text{ k}\Omega$ , so the impedance at 1 kHz was reduced by a factor of 21.

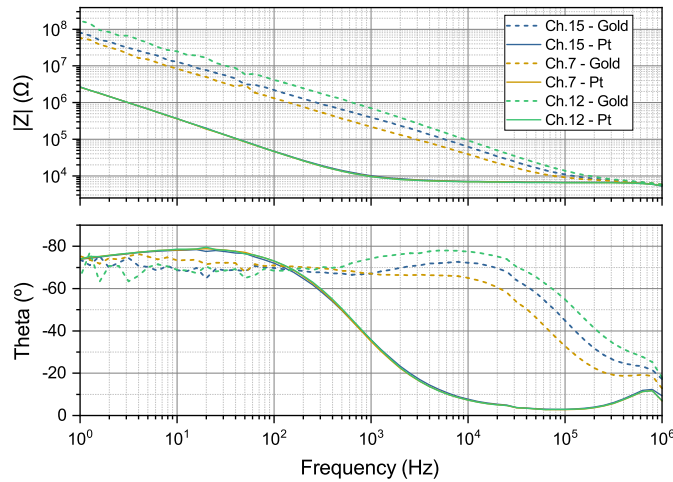


Fig. 7. Comparison of the results obtained before and after platinization process. Is shown the bode diagram including magnitude and phase. Results shown a decrease in the impedance of the electrodes after coating.

From the figure it can be seen that the value of  $R_s$  (value reached at the flat zone at high frequencies) was maintained even when platinization was applied, given that it depended mainly on the conduction of the electrolyte itself and not on the electrode-electrolyte interface. Finally, it should be noted that the curves begin to behave in a random way at frequencies close to 1 MHz due to the limits of the measuring equipment.

### B. Noise analysis / SNR

Noise analysis was based on the different noise contributions, as mentioned in section II. The study of noise was focused on the thermal noise that appears in the system related to the movement of electrons due to thermal agitation and the noise contribution of the device.

The liquid-metal interface adds noise to the system that affects at the range of the electrophysiological signals. Note that the increasing of the size of the microelectrodes results in an decrease in their impedance [9]. The real part of the impedance of each electrode was the major contributor to this type of noise known as thermal noise that can be calculated as follows:

$$v_n = \sqrt{4kTR\Delta f} \quad (2)$$

where  $k$  is the Boltzmann constant,  $T$  is the absolute temperature (in  $K$ ),  $R$  is the real part of the resistance of the electrode, and  $\Delta f$  is the recorded frequency range.

The results of the analysis are shown in Table I, including the value of the mean and standard deviation of the 16 channels (8 for each MEA).  $|Z|$  is the magnitude of the electrode impedance measured at 1 kHz;  $R_s$  is the resistance at phase angle zero; thermal noise is calculated for a frequency value close to  $10^5 \text{ Hz}$ ; RMS noise, calculated in the frequency range between 100 Hz and 1500 Hz, is defined as the equation 3.

$$v_{rms} = \sqrt{4kT \int_{f_0}^{f_1} |Z(f)| df} \quad (3)$$

TABLE I  
RESULTS OF COATING ELECTRODES FROM EIS CHARACTERIZATION

Parameter	Unit	Value
$ Z $ (at 1 kHz)	$\text{k}\Omega$	$10.26 \pm 1.075$
$R_s$	$\text{k}\Omega$	$6.466 \pm 0.396$
Thermal Noise	$\mu\text{V}$	$3.2617 \pm 0.101$
RMS Noise	$\mu\text{V}$	$0.5559 \pm 0.072$

Aspects related to  $R_s$  and  $|Z|$  measured at 1 kHz have been already discussed in previous sections. Thermal noise is the electronic noise generated by the thermal agitation of the charge carriers inside an electrical conductor at equilibrium, which occurs independently of any applied voltage and is directly related to the square root of the impedance of the electrode. Therefore, by decreasing the impedance, the thermal noise should decrease.

The discussion about RMS noise is similar but taking into account the frequency range of interest for the application, between 100 Hz and 1500 Hz in our case, fitting the impedance curve using an exponential ( $a \cdot e^{b/(x+c)}$ , where  $a=6478.45$ ,  $b=462.68$ ,  $c=135.92$ ) and calculating the corresponding integral.

To compare the theoretical and experimental results, a recording of the noise in the system was acquired using a simple setup where the MEA was introduced into the electrolyte without any external excitation or cardiac sample. The experimental results were  $87.7 \mu\text{V}$  for thermal noise and  $6.5 \mu\text{V}$  for RMS noise, while the theoretical results are shown in Table I. These results indicate that the experimental noise presents higher values due to the electromagnetic noise (EMI)

existing in the working environment, making it impossible to appreciate the variation that occurs in the thermal noise when the impedance is modified.

To conclude, we verified that the impedance matching between the electrode and the amplifier was adequate since the selected amplifier has an input impedance of 1300 M $\Omega$  at 10 Hz, while the value of the electrode impedance does not exceed 2 M $\Omega$ . At 1 kHz, the operational amplifier has 13 M $\Omega$  and the electrode presents 10 k $\Omega$ . This will enable the correct acquisition of the signals from the cardiac tissues.

#### IV. CONCLUSIONS

MEAs were characterized, validating a part of the FP measurement system. A potentiostat and an electrochemical interface were used to adjust the characteristic curve of the electrodes by depositing black platinum on the measurement points. After platinization, improved behavior of the electrodes was obtained based on impedance results, with all MEA channels showing uniform behavior.

The election of the electrolyte for characterization is essential, as the value at which the curve stabilises at high frequencies is dependent on the liquid in which the electrodes are soaked. Experiments were performed at 10 mM PBS since this is the medium selected for future FP measurements from human cardiac samples.

With the decrease of the impedance by more than 20 times, especially at low and medium frequencies, we obtained improved quality of the signals that reach the input of the amplifier due to the existing ratio in the divider formed by the impedance of the electrode and the input impedance of the operational amplifier. This can mean that reducing the absolute electrode impedance through Pt-black deposition, the signal-attenuation effect was reduced to < 2% for a 50  $\mu$ m electrode size [8].

#### ACKNOWLEDGMENT

This work was funded by projects PID2019-105674RB-I00 by Ministerio de Ciencia e Innovación, ERC grant 638284 by European Research Council and project LMP94\_21 and BSICoS group T39\_20R by European Social Fund (EU) and Aragón Government.

#### REFERENCES

- [1] Stefan R. Braam, Leon Tertoolen, Anja van de Stolpe, Thomas Meyer, Robert Passier, and Christine L. Mummery. Prediction of drug-induced cardiotoxicity using human embryonic stem cell-derived cardiomyocytes. *Stem Cell Research*, 4:107–116, 3 2010.
- [2] Udo Kraushaar and Elke Guenther. Assay procedures for compound testing of hiPSC-derived cardiomyocytes using multiwell microelectrode arrays. *Methods in Molecular Biology*, 1994:197–208, 2019.
- [3] Cellular Physiology, Alexandra Bussek, Erich Wettwer, Torsten Christ, Horst Lohmann, Patrizia Camelliti, and Ursula Ravens. Cellular physiology cellular physiology cellular physiology cellular physiology tissue slices from adult mammalian hearts as a model for pharmacological drug testing, 2009.
- [4] Michele Dipalo, Sahil K Rastogi, Laura Matino, Raghav Garg, Jacqueline Bliley, Giuseppina Iachetta, Giovanni Melle, Ramesh Shrestha, Sheng Shen, Francesca Santoro, Adam W Feinberg, Andrea Barbaglia, Tzahi Cohen-Karni, and Francesco De Angelis. Intracellular action potential recordings from cardiomyocytes by ultrafast pulsed laser irradiation of fuzzy graphene microelectrodes, 2021.
- [5] Alfred Stett, Ulrich Egert, Elke Guenther, Frank Hofmann, Thomas Meyer, Wilfried Nisch, and Hugo Haemmerle. Biological application of microelectrode arrays in drug discovery and basic research. *Analytical and Bioanalytical Chemistry*, 377:486–495, 2003.
- [6] Leonardo D. Garma, Laura Matino, Giovanni Melle, Fabio Moia, Francesco De Angelis, Francesca Santoro, and Michele Dipalo. Cost-effective and multifunctional acquisition system for in vitro electrophysiological investigations with multi-electrode arrays. *PLoS ONE*, 14:1–13, 2019.
- [7] Patrizia Camelliti, Sara Abou Al-Saud, Ryszard T. Smolenski, Samha Al-Ayoubi, Alexandra Bussek, Erich Wettwer, Nicholas R. Banner, Christopher T. Bowles, Magdi H. Yacoub, and Cesare M. Terracciano. Adult human heart slices are a multicellular system suitable for electrophysiological and pharmacological studies. *Journal of Molecular and Cellular Cardiology*, 51:390–398, 2011.
- [8] Vijay Viswam, Marie Engelen J. Obien, Felix Franke, Urs Frey, and Andreas Hierlemann. Optimal electrode size for multi-scale extracellular-potential recording from neuronal assemblies. *Frontiers in Neuroscience*, 13, 2019.
- [9] David A Robinson. The electrical properties of metal microelectrodes. *Proceedings of the IEEE*, 56(6):1065–1071, 1968.
- [10] Marie Engelen J. Obien, Kosmas Deligkaris, Torsten Bullmann, Douglas J. Bakkum, and Urs Frey. Revealing neuronal function through microelectrode array recordings. *Frontiers in Neuroscience*, 9:423, 2015.
- [11] Aida Oliván-Viguera, María Pérez-Zabalza, Laura García-Mendivil, Konstantinos A Mountris, Sofía Orós-Rodrigo, Estel Ramos-Marquès, José María Vallejo-Gil, Pedro Carlos Fresneda-Roldán, Javier Fañanás-Mastral, Manuel Vázquez-Sancho, et al. Minimally invasive system to reliably characterize ventricular electrophysiology from living donors. *Scientific reports*, 10(1):1–13, 2020.
- [12] Alex Suarez-Perez, Gemma Gabriel, Beatriz Rebollo, Xavi Illa, Anton Guimerà-Brunet, Javier Hernández-Ferrer, María Teresa Martínez, Rosa Villa, and María V. Sanchez-Vives. Quantification of signal-to-noise ratio in cerebral cortex recordings using flexible MEAs with co-localized platinum black, carbon nanotubes, and gold electrodes. *Frontiers in Neuroscience*, 12, 11 2018.
- [13] Gergely Márton, István Bakos, Zoltán Fekete, István Ulbert, and Anita Pongrácz. Durability of high surface area platinum deposits on microelectrode arrays for acute neural recordings. *Journal of Materials Science: Materials in Medicine*, 25:931–940, 2014.
- [14] Sverre Grimnes and Ørjan G Martinsen. Data and models. *Bioimpedance and Bioelectricity Basics*, pages 329–404, 1 2015.
- [15] Sharanya Arcot Desai, John D. Rolston, Liang Guo, and Steve M. Potter. Improving impedance of implantable microwire multi-electrode arrays by ultrasonic electroplating of durable platinum black. *Frontiers in Neuroengineering*, 3:1–11, 2010.
- [16] Stuart F. Cogan. Neural stimulation and recording electrodes. *Annual Review of Biomedical Engineering*, 10:275–309, 2008.